Dark Matter Annihilation around Intermediate Mass Black Holes: an update

Gianfranco Bertone [a], Mattia Fornasa[b], Marco Taoso[b] & Andrew R. Zentner[c]
[a] *Institut d'Astrophysique de Paris, UMR 7095-CNRS*
Université Pierre et Marie Curie, Bd Arago 98bis, 75014 Paris
[b] *University of Padova & INFN sezione di Padova, via Marzolo 8, 35131 Padova, Italy*
[c] *Dept. of Physics and Astronomy, University of Pittsburgh, Pittsburgh, PA 15260 USA*

The formation and evolution of Black Holes inevitably affects the distribution of dark and baryonic matter in the neighborhood of the Black Hole. These effects may be particularly relevant around Supermassive and Intermediate Mass Black Holes (IMBHs), the formation of which can lead to large Dark Matter overdensities, called *spikes* and *mini-spikes* respectively. Despite being larger and more dense, spikes evolve at the very centers of galactic halos, in regions where numerous dynamical effects tend to destroy them. Mini-spikes may be more likely to survive, and they have been proposed as worthwhile targets for indirect Dark Matter searches. We review here the formation scenarios and the prospects for detection of mini-spikes, and we present new estimates for the abundances of mini-spikes to illustrate the sensitivity of such predictions to cosmological parameters and uncertainties regarding the astrophysics of Black Hole formation at high redshift. We also connect the IMBHs scenario to the recent measurements of cosmic-ray electron and positron spectra by the PAMELA, ATIC, H.E.S.S., and Fermi collaborations.

PACS numbers:

I. INTRODUCTION

The distribution of matter around a Black Hole (BH) is inevitably affected by its formation and evolution, both in the case of baryons [1, 2] and Dark Matter (DM) [3]. The physics is relatively simple: when a compact object forms, the surrounding matter reacts to the increased gravitational potential, and if the growth proceeds on a timescale much longer than the dynamical time of the system, large overdensities can be achieved. This is particularly important for the DM distribution, because the DM annihilation rate is proportional to the square of the number density of DM particles. This means that if BH formation increases the DM density locally, it also boosts the annihilation rate and improves the prospects for detecting DM through the observation of secondary particles such as gamma-rays, anti-matter and neutrinos.

Gondolo and Silk have applied this argument to the distribution of DM at the center of the Galaxy [3], where a Supermassive BH (SMBH) of 2–4 $\times 10^6 M_\odot$ is known to dominate the gravitational potential within a sphere of radius $r_h \sim 1$ pc. The consequent enhancement in the DM density around the central SMBH (dubbed a *spike*) was subsequently shown likely to be reduced by major merger events, off-center formation of the seed BH, gravitational scattering off stars and DM annihilations [4, 5, 6, 7]. Zhao and Silk have subsequently suggested that mild overdensities of DM could also be present around Intermediate Mass Black Holes (IMBHs), remnants of Pop III stars, and provided the first rough estimates of the properties of *mini-spikes* surrounding IMBHs in the Milky Way [8].

Bertone, Zentner and Silk (hereafter BZS) built a consistent formation and evolution scenario for IMBHs and associated mini-spikes, for two different classes of models: "mild" mini-spikes around IMBHs remnants of Pop III stars, and "strong" mini-spikes, around more massive compact objects [9]. For both scenarios, BZS tracked the merger history of each individual BH, and selected precisely those IMBHs which never experienced mergers, to ensure at a minimum that major mergers have not destroyed any spike that may have existed around the original BH. This has allowed a detailed quantitative description of the mini-spikes scenario, and practically all subsequent studies published in the literature have made use directly or indirectly of the BZS IMBH models. Moreover, BZS were able to predict some of the demographics of wandering IMBHs, that may not be directly associated with the Milky Way bulge or disk, and they proposed to search for a class of gamma-rays objects sharing the same energy spectrum as a smoking-gun signature of DM annihilations.

Here, we review the formation scenarios and the physics behind the BZS IMBH models, and explore how the population of IMBHs, thus of mini-spikes, depends on cosmological, astrophysical and particle physics parameters. To this aim, we update the original BZS catalogs, including the most recent determination of cosmological parameters, and explore the dependence on astrophysical quantities.

We also review here the experimental strategies that may allow the detection of mini-spikes, including the observation of multiple gamma-ray and neutrino sources in the Milky Way, a collection of gamma-ray sources around M31, and the possible contribution to the absolute flux and the angular power spectrum of the Extra-galactic Gamma-ray Background (EGB).

The paper is organized as follows: in Section II, we review the IMBHs formation scenarios and discuss the current population of IMBHs in the Milky Way. In Section III we discuss adiabatic contraction and the formation of mini-spikes. Section IV is dedicated to the prospects for

detecting DM through gamma-rays and neutrinos from IMBHs in our Galaxy and in M31. In Section V we discuss the impact of the mini-spikes population on the Extra-galactic Gamma-ray Background. In the final section (Section VI) we discuss our results and present our conclusions.

II. INTERMEDIATE MASS BLACK HOLES

A. Hints for detection of IMBHs

We refer to BHs with masses within a relatively large range, $100 M_\odot \lesssim M \lesssim 10^6 M_\odot$ as Intermediate Mass Black Holes. The lower limit is roughly the mass of the largest BH that can be produced by stellar collapse [11], and the upper limit corresponds to the minimum mass for a SMBH. There is not a clear experimental evidence for this class of objects, but they are often invoked as an explanation of Ultra Luminous X-ray sources, i.e. sources that emit at a luminosity larger than 10^{39}erg s^{-1}, thus exceeding the Eddington luminosity of stellar BHs [12].

IMBHs may also be hosted inside globular clusters [13]. A hint in favor of this possibility comes from the fact that the predicted masses for the IMBHs and the velocity dispersion typical of a globular cluster follow exactly the extrapolation at lower values of the $M_\bullet - \sigma$ relation valid for SMBHs [14].

From a theoretical point of view, IMBHs may provide massive enough seeds for the growth of high-redshift SMBHs, as observed by the Sloan Digital Sky Survey in the form of quasars at redshifts as high as $z \sim 6$ [15, 16, 17]. Conclusive evidence for IMBHs may come in the near future from the detection (e.g. by LISA [18]) of the gravitational waves emitted in the mergers of IMBHs [19, 20, 21].

B. Formation

In BZS, two formation scenarios for IMBHs have been studied, and we refer to that paper for a detailed discussion. In the first scenario (scenario A) IMBHs are remnants of the collapse of Population III stars [22]. Since the Jeans mass scales with the temperature as $T^{3/2}$, the mass of Pop III stars (which form early in a hot environment) is expected to be higher than other stars, around $150 - 200\ M_\odot$ [23, 24]. Newtonian simulations suggest that the evolution of Pop III stars is very different from stars in the local Universe. Zero metallicity Pop III stars evolve on a timescale of order $t_* \sim 1 - 10$ Myr. If their masses are in the range $M \sim 60 - 140 M_\odot$ and $M \gtrsim 260 M_\odot$, they collapse directly to BHs, while if $140 \lesssim M/M_\odot \lesssim 260 M_\odot$, they are completely disrupted due to the pulsation-pair-production instability, leaving behind no remnant [25] (see also Refs. [26, 27, 28, 29]).

The second formation scenario (scenario B) considered by BZS was based on Ref.[30], as an example of models in which the collapse of primordial gas in early-forming halos leads to the "direct" formation of very massive objects [31, 32, 33, 34, 35, 36]. In this specific scenario, the baryons in the low tail of the angular momentum distribution form a pressure-supported disc at the center of the halo. Gravitational instabilities then turn on an effective viscosity that make baryons lose their angular momentum, causing an inward mass flow. The process comes to an end after $1 - 30$ Myr, when the first stars form or when the halo experiences a major merger [30]. The central object will then undergo gravitational collapse producing the final BH.

The requirement that loss of angular momentum via viscosity is effective, fixes a mass scale of $10^7 - 10^8 M_\odot$ for the initial halos, and leads to a mass scale for the final IMBHs of order $10^5 M_\odot$. In fact, the mass distribution for scenario B turns out to be a log-normal Gaussian ($\sigma_\bullet = 0.9$) with a mean value $M_\bullet$:

$$M_\bullet = 3.8 \times 10^4 M_\bullet \left(\frac{\kappa}{0.5}\right) \left(\frac{f}{0.03}\right)^{3/2} \left(\frac{M_{vir}}{10^7 M_\odot}\right) \left(\frac{1+z_f}{18}\right) \left(\frac{t}{10\ \mathrm{Myr}}\right), \quad (1)$$

where M_{vir} is the virial mass of the halo, z_f the redshift of formation, f the fraction of the baryonic mass of the halo that goes into the central pressure-supported disc, κ the fraction of the mass of the disc that ends up in the final IMBH and t is the timescale available for angular momentum transfer due to the effective viscosity.

BZS have estimated the population of IMBHs in the MW in scenario A as follows: they populated all the halos at $z = 18$ that constitute a 3σ peak (with respect to the average density) with a pristine IMBH of mass 100 $M_\odot$. The evolution of the halos is then simulated as in Refs. [19, 37, 38, 39], a procedure that tracks the growth and mergers of the structures down to redshift zero. The IMBHs in the halos that never experience mergers survive until the present epoch and constitute the current population of scenario A IMBHs. Their mass is assumed to remain unchanged with respect to the initial value $\sim 100\ M_\odot$, and the number of unmerged IMBHs was found to be $N_A = (1027 \pm 84)$.

In the case of scenario B, BZS have followed a similar approach for the evolution of IMBHs, with the difference that only those halos with a mass larger than the mass threshold M_{thr} for the onset of the effective viscosity (see the discussion above) are populated with IMBHs, with a mass function as in Eq. 1 (see also Fig. 1). The predicted number of IMBHs in the MW for scenario B was $N_B = (101 \pm 22)$ [9] (see below for more recent results obtained with updated cosmological parameters).

Each of these models of high-redshift seed BH formation is reasonable, but both of these scenarios remain uncertain in their detail. In particular, these models exhibit parameters that may reasonably take on a wide range of values leading to markedly different predictions for IMBH demographics at $z = 0$. The formation of seed

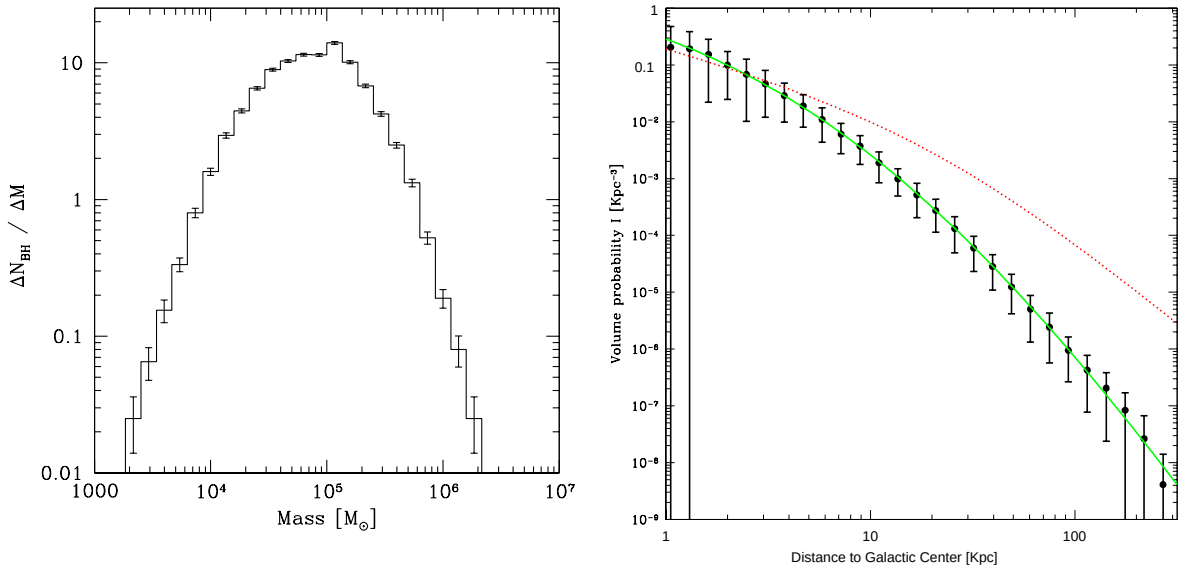

FIG. 1: *Left:* Mass function of unmerged IMBHs in the scenario B for a MW halo at $z = 0$. The distribution is based on the average of 200 Monte Carlo realizations of a halo of virial mass $M_{vir} = 10^{12.1} h^{-1} M_{\odot}$, roughly the size of the halo of the MW. Taken from Ref. [9]. *Right:* Radial distribution of the IMBH population in the MW from the numerical simulation of Ref. [9]. The points refers to the average among 200 Monte Carlo realizations of the MW halo and the error bars show the scatter among realizations. The solid line is the analytical fit and the dotted line is a NFW profile. Taken from Ref. [10].

BHs in both scenarios is cut off at redshifts when significant small-scale fragmentation of baryonic disks sets in and BH formation in scenario B terminates absolutely when the Universe becomes significantly reionized. In what follows we exhibit the significant parameter freedom within these models by varying the formation redshift in scenario A, and the reionization redshift in scenario B among viable and illustrative values. In scenario A, lowering the formation redshift requires that the seed black holes generally form in halos of higher mass, leading to reduced abundance, while in scenario B lowering the redshift of reionization allows angular momentum loss to be effective for a longer period, increasing the number of seed black holes. We note here that the range of parameters we choose are currently viable and refer the reader to BZS for modeling details.

The radial distribution of IMBHs was found to be steeper than a Navarro-Frenk-White (NFW) profile [40] (see the right panel of Fig. 1), and it is well fitted by the following analytical function [10]:

$$N(r) = 5.96 \times 10^{-2} \left[1 + \left(\frac{r}{9.1 \text{ kpc}} \right)^{0.51} \right]^{-10.8} \text{kpc}^{-3}. \quad (2)$$

III. ADIABATIC CONTRACTION

As mentioned in the introduction, IMBHs and SMBHs are particularly interesting for indirect DM searches, because they may act as *annihilation boosters*, as their growth can lead to large DM overdensities that enhance annihilation fluxes (see e.g. Ref. [41] for a review). In particular, if the crossing timescale t_{cr} (the time needed for a DM particle to cross the central part of the halo) is much smaller than the BH growth timescale t_{growth}, DM particles conserve their angular momenta and their radial actions (the integral of the radial velocity over one closed orbit), and move to orbits which are closer to the BH, thus enhancing their number density and annihilation rate.

The first study of adiabatic contraction was performed by Young in 1980 [2] in the context of stellar systems. In subsequent studies also DM has been taken into account [42, 43, 44] and two different situations have usually been considered:

- "analytical cores", in which case the initial DM profile can be Taylor-expanded around the BH as: $\rho_{\chi}(r) \approx \rho_{\chi,0} + 1/2 \rho''_{\chi,0} r^2 + \mathcal{O}(r^3)$,
- γ-models, in which the inner initial DM profile is a power-law, $\rho_{\chi}(r) \propto r^{-\gamma}$.

The result of the adiabatic contraction is different in the two cases. A strong density enhancement, or *spike*, is produced in both cases, but the final slope is steeper for

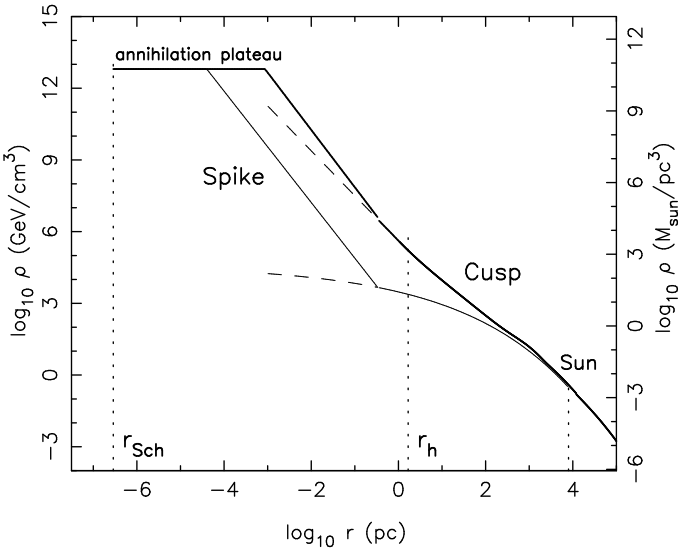

FIG. 2: Possible models for the DM distribution in the Galaxy. The thin curve shows the standard halo model, and the thick curve is the same model after "adiabatic compression" by the Galactic baryons (stars and gas). Both curves are normalized to a DM density of 0.3 GeV cm^{-3} at the Solar circle. Curves labeled "spike" show the increase in density that would result from growth of a Galactic SMBH at a fixed location. The annihilation plateau, $\rho = \rho_a = m/\langle\sigma v\rangle t$, was computed assuming $m = 200$ GeV, $\langle\sigma v\rangle = 10^{-28}$ cm^3 s^{-1} and $t = 10^{10}$ yr. Dotted vertical lines indicate the SMBH Schwarzschild radius ($r_{Sch} \approx 2.9 \times 10^{-7}$ pc, assuming a mass of $3.0 \times 10^6 M_\odot$ and zero rotation), the SMBH gravitational influence radius ($r_h \approx 1.7$ pc), and the radius of the Solar circle ($R_\odot \approx 8.0$ kpc). Effects of the dynamical processes (scattering of DM off stars, loss of DM into the SMBH, etc.) are excluded from this plot; these processes would generally act to decrease the DM density below what is shown here, particularly in the models with a "spike.". Taken from [7].

γ-models. The difference is due to the different behavior of the phase-space distribution function $f(E,t)$. In the case of γ-models, f diverges in the limit $E \to \Phi(0)$, meaning that cold orbits (those orbits populated by particles with very low velocities) have a large occupation number. The final DM profile for a γ-model is a new power-law $\rho_\chi \propto r^{-\gamma_{sp}}$ with a steeper slope. The value of γ_{sp} depends on the initial slope as in the following equation:

$$\gamma_{sp} = \frac{9 - 2\gamma}{4 - \gamma}. \tag{3}$$

The effect of SMBH growth at the Galactic center on DM density profiles is shown in Fig. 2 for an initial NFW profile ($\gamma = 1$). The final profile in this case is a power-law of index $\gamma_{sp} = 7/3$ within a region of radius $r_{sp} \sim 0.2 r_h$, where r_h is the radius that encloses a DM mass equal to twice the mass of the central BH.

There is an upper limit to the DM density that can be achieved around the SMBH (see Fig. 2). In fact, the power-law solution is valid only down to a radius equal to the last stable orbit around the SMBH and, furthermore, DM annihilation itself sets an upper limit on the DM density of order $m_\chi/\sigma v(t - t_f)$, so that the density is saturated at a cut-off radius of

$$r_{cut} = \mathrm{Max}\left[4R_{\rm Schw}, r_{\rm lim}\right], \tag{4}$$

where $R_{\rm Schw}$ is the Schwarzschild radius of the IMBH $R_{\rm Schw} = 2.95\,\mathrm{km}\,(M_{\rm bh}/\,\mathrm{M}_\odot)$.

Any spike forming at the center of a galactic halo would inevitably be affected by dynamical processes that tend to deplete the DM density [4, 5, 6]. For instance, a merger between two halos, the interaction with a globular cluster or the presence of a bar are all able to disrupt the distribution of the cold particles that constitute the spike, efficiently damping the enhancement [4, 5]. Furthermore, the BH may not form exactly at the center of the DM distribution [4], in which case the orbits that the BH crosses in its spiraling in will be depleted and the final enhancement will be much shallower than depicted in Fig. 2. Finally, one should also take into account the interactions of the DM particles with baryons [5]: transferring energy to the DM particles, the effect is, as before, of heating the DM so that the particles in the spike will be able to leave the central region. When also including the effect of DM annihilations, it is possible to show that any DM overdensity around a BH at the center of a galactic halo can hardly survive until today [6], although interactions of baryons can actually lead to the re-growth of mild overdensities known as DM *crests* [45]. Our approach is to account for some of these mitigating factors by considering only those BHs that formed at high redshift and were found never to interact with any other BH during the hierarchical merging process, as discussed in Ref. [9]. Moreover, at least for scenario B, off-center formation is not possible for IMBHs and interactions of DM with baryons have only minor effects, so that, in contrast

to SMBHs, IMBHs can effectively retain their mini-spike.

IV. DETECTION OF DM AROUND IMBHS

The flux of secondary particles produced by DM annihilation around an IMBH can be written as

$$\frac{d\Phi}{dE}(E) = \frac{\langle\sigma v\rangle}{8\pi m_\chi^2}\frac{dN_\gamma}{dE}(E)\int \rho_{sp}^2(r)dV\,, \qquad (5)$$

where $\langle\sigma v\rangle$ is the thermally-averaged annihilation cross section, m_χ is the mass of the DM particle and dN_γ/dE is the number of secondary particles produced per annihilation. The integral extends from the *cut radius* r_{cut} (i.e. the radius where the DM density reaches the annihilation plateau in Fig. 2) to the spike radius r_{sp}. Inserting the appropriate reference values, Eq. 5 can be recast as

$$\begin{aligned}\frac{d\Phi}{dE}(E) \;=\; & \Phi_0\frac{dN_\gamma}{dE}\left(\frac{\langle\sigma v\rangle}{10^{-26}\mathrm{cm^3 s^{-1}}}\right)\left(\frac{m_\chi}{100\ \mathrm{GeV}}\right)^{-2} \\ & \left(\frac{d}{\mathrm{kpc}}\right)^{-2}\left(\frac{\rho_{sp}(r_{sp})}{10^2\ \mathrm{GeV\ cm^{-3}}}\right)^2\left(\frac{r_{sp}}{\mathrm{pc}}\right)^{14/3} \\ & \left(\frac{r_{cut}}{10^{-3}\mathrm{pc}}\right)^{-5/3}\,, \end{aligned} \qquad (6)$$

with $\Phi_0 = 9\times10^{-10}\mathrm{cm^{-2}s^{-1}}$, a normalization factor that makes it evident that IMBHs can be bright DM annihilation sources, possibly as bright as the entire MW.

The fact that the cut radius itself depends on the mass and the cross section of the DM candidate alters the naïve dependence of the annihilation flux from these quantities, and it is easy to show that in this case $d\Phi/dE \propto \langle\sigma v\rangle^{2/7} m_\chi^{-9/7}$. The weak dependence of the predicted annihilation flux on the particle physics parameters is one of the intriguing features of the mini-spikes scenario.

In Figs. 3 and 4 the number of IMBHs associated with a gamma-ray flux (integrated above 1 GeV) larger than Φ is plotted as a function of Φ itself. With respect to the similar Figs. 4 and 5 in Ref. [9], we consider here the most recent cosmological parameters from WMAP5, and find a significant decrease of the number of IMBHs . In order to show the effect of changing the cosmological parameters we have considered two representative values of the redshift of formation z_f for the scenario A and we have varied the reionization redshift z_r for the scenario B in the WMAP5 3σ range [46]. The total number of IMBHs for the different choices of astrophysical parameters is shown in Table I.

Figs. 3 and 4 can also be loosely interpreted as the number of objects that can be detected with an experiment of sensitivity Φ. For EGRET, $\Phi_{EGRET} \approx 3\times10^{-8}\mathrm{cm^{-2}s^{-1}}$, while for Fermi $\Phi_{Fermi} \approx 3\times10^{-10}\mathrm{cm^{-2}s^{-1}}$. The fact that the scenario is within the reach of EGRET, means that some of the unidentified EGRET sources could be interpreted as IMBHs.

Scenario	z	N_{BH}	1σ scatter
A	18	319	49
A	15	54	13
B	7	278	37
B	12	62	14
B	17	8.4	3.7

TABLE I: Number of unmerged IMBHs in a Milky-Way like halo at $z = 0$. The four columns indicate the formation scenario, the formation (reionization) redshift in the case of scenario A (B), the number of IMBHs and the 1σscatter among realizations

.

If this interpretation was confirmed by Fermi, which is expected to see many more sources, the identification of a population of point-like sources with the same energy spectrum would provide strong evidence for a DM annihilation signal. We stress that the number of detectable sources depend on the formation scenario but also on other poorly constrained processes, such as the merger history of IMBHs in the galaxy and the initial distribution and dynamical evolution of the surrounding DM. Furthermore, from a particle physics point of view, we recall that the DM annihilation cross section can largely differ from the thermal value in presence of efficient coannihilations [47], significant Sommerfeld enhancements [48, 49, 50, 51], in cases where DM particles are not thermal relics, or in non-standard cosmological scenarios [52, 53, 54].

Even in the conservative case where none of the EGRET sources is associated with a mini-spike, there are models where the Fermi satellite may detect this class of objects, do to the steep decline of the luminosity function in Figs. 3 and 4.

The first experimental constraints on the mini-spikes scenario have been obtained through a survey of the inner Galactic plane at photon energies above 100 GeV performed by the H.E.S.S. array of Cherenkov telescopes from 2004 to 2007 [55]. About 400 hours of data have been accumulated in the region between -30 and +60 degrees in Galactic longitude, and between -3 and +3 degrees in Galactic latitude, and a H.E.S.S. sensitivity map was computed for DM annihilations. The data exclude scenario B at a 90% confidence level for DM particles with velocity-weighted annihilation cross section $\sigma v \gtrsim 10^{28}$ cm^3 s^{-1} and mass between 800 GeV and 10 TeV.

As for the prospects for detecting mini-spikes with the Fermi telescope, a dedicated analysis of the minimum detectable annihilation flux has been presented in Ref. [56] and further discussed in the pre-launch estimates of the Fermi sensitivity to DM annihilation signals [57]. The mock IMBH catalogs obtained for the Milky Way have been adapted, by a suitable rescaling, to the population of IMBHs hosted by the Andromeda galaxy [58], leading to the prediction that the M31 should host about

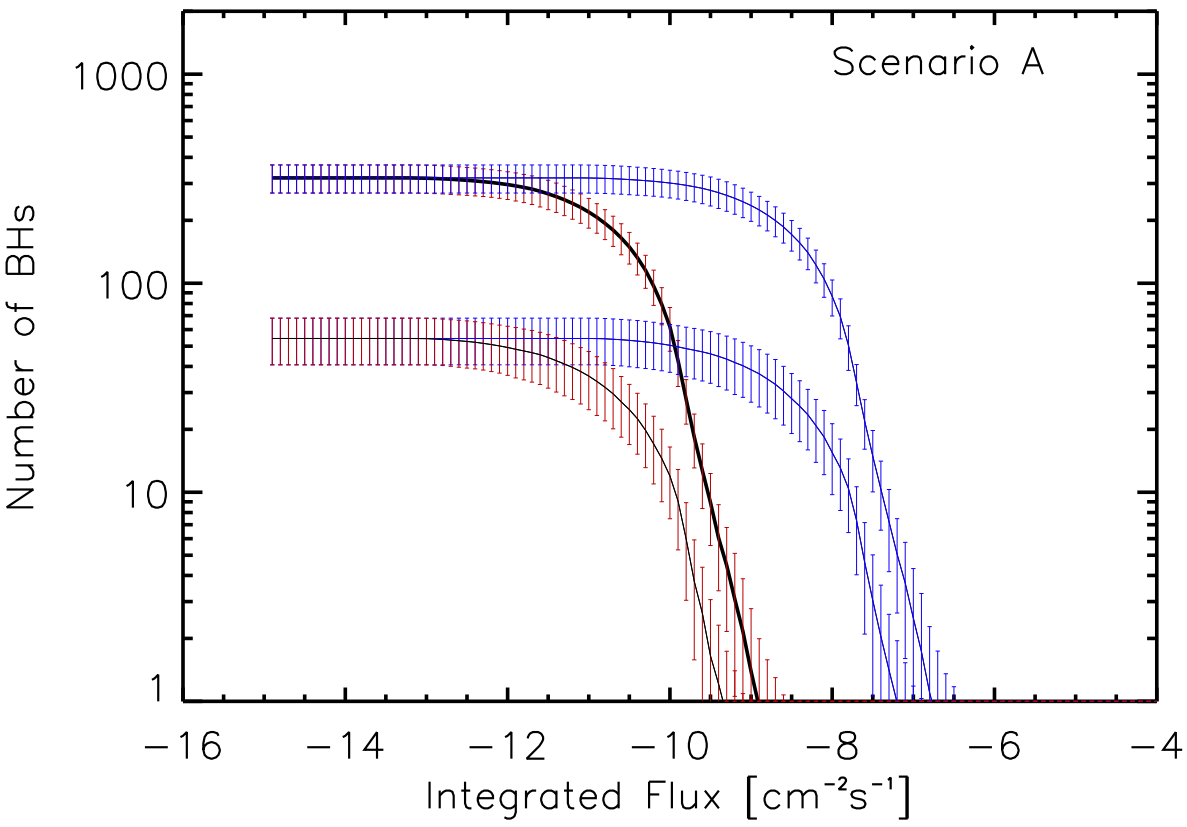

FIG. 3: IMBHs integrated luminosity function, i.e. number of IMBHs producing a gamma-ray flux larger than a given flux Φ (above 1 GeV), as a function of Φ, for scenario A. For each curve we also show the 1σ scatter among the different realization of the Milky Way-size host DM halo. The blue (red) curve refers to a DM particle with a mass of 100 GeV (1 TeV) and a cross section of $\langle\sigma v\rangle = 3\times10^{-26}\mathrm{cm}^{-3}\mathrm{s}^{-1}$ ($\langle\sigma v\rangle = 3\times10^{-29}\mathrm{cm}^{-3}\mathrm{s}^{-1}$) . The upper (lower) set of lines corresponds to a redshift of formation $z_f = 18$ (15). The figure can be interpreted as the number of IMBHs detectable by experiments with a point source sensitivity Φ (above 1 GeV) as a function of Φ.

65 IMBHs (again this estimate strongly depends on the assumed cosmological parameters). Detectability toward Andromeda is reduced greatly due to the comparably large distance to the Andromeda galaxy. On the other hand, in the case of detecting a handful of such objects, they will all be located within $\sim 3^\circ$ from the center of Andromeda, which may be an interesting spatial signature (see Fig. 5).

A. Neutrinos from IMBHs

DM annihilation can also produce neutrinos, both directly or through the decay of secondary particles. Being strong annihilation "boosters", IMBHs may also be bright neutrino sources [59, 60], which can be detected by high energy neutrino telescopes such as ANTARES and IceCube or the future Km3. Neutrino telescopes detect neutrinos through the observation of muons produced by charged current interactions of neutrinos with the nuclei around the detector. Accounting for oscillations we can write the muon flux as:

$$\frac{d\Phi_{\nu_\mu}}{dE}(E) = \frac{\langle\sigma v\rangle}{8\pi m_\chi^2}\int\rho^2(r)dV \sum_{\ell\in\{e,\mu,\tau\}}\mathcal{P}(\nu_\ell\to\nu_\mu)\frac{dN_{\nu_\ell}}{dE}(E), \quad (7)$$

where $\mathcal{P}(\nu_\ell \to \nu_\mu)$ is the probability of having a muon neutrino at the detector when at the source a neutrino of the ℓ family is produced, and it can be written in terms of the oscillation matrix U: $\mathcal{P}(\nu_\ell\to\nu_\mu) = \sum_{j\in\{e,\nu,\tau\}}|U_{\ell j}|^2|U_{\mu j}|^2$.

Finally, the rate of events in a neutrino telescope is

$$R = \int_{E_\mu^{thr}}^{m_\chi} dE_\nu \int_0^{y_\nu} dy A(E_\mu)P_\mu(E_\nu,y)\frac{dN_\nu}{dE_\nu}(E_\nu), \quad (8)$$

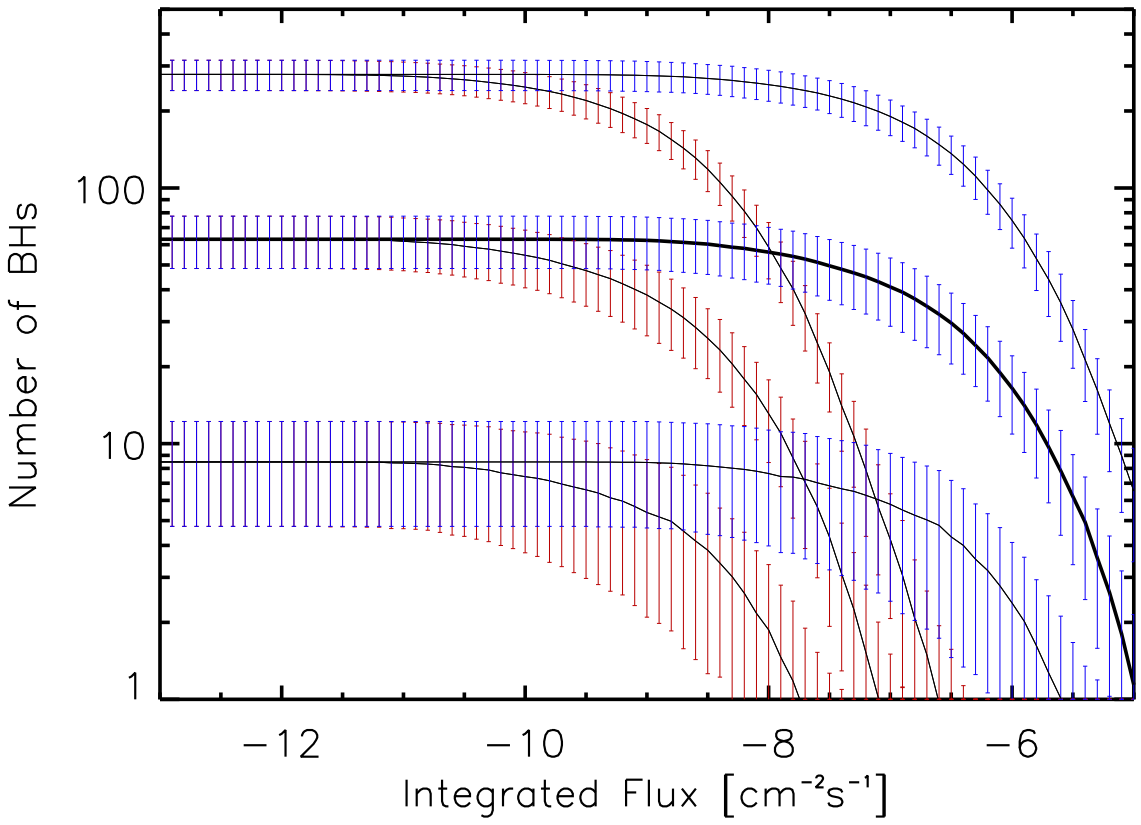

FIG. 4: IMBHs integrated luminosity function, i.e. number of IMBHs producing a gamma-ray flux larger than a given flux Φ (above 1 GeV), as a function of Φ, for scenario B. For each curve we also show the 1σ scatter among the different realization of the Milky Way-size host DM halo. The blue (red) curve refers to a DM particle with a mass of 100 GeV (1 TeV) and a cross section of $\langle\sigma v\rangle = 3\times10^{-26}\mathrm{cm}^{-3}\mathrm{s}^{-1}$ ($\langle\sigma v\rangle = 3\times10^{-29}\mathrm{cm}^{-3}\mathrm{s}^{-1}$) . The middle (upper, lower) set of lines corresponds to a redshift of reionization $z_r = 12$ (7, 17). The figure can be interpreted as the number of IMBHs detectable by experiments with a point source sensitivity Φ (above 1 GeV) as a function of Φ.

where $y_\nu = 1 - E_\mu^{thr}/E_\nu$, E_μ^{thr} is the experimental threshold for muons, $A(E_\mu)$ is the effective area and $P_\mu(E_\nu, y)$ is the probability that a muon neutrino interacts with a nucleon producing a muon of energy $E_\mu = (1-y)E_\nu$ (see Ref. [59] for details). Results are summarized in Fig. 2 of Ref. [59], similar to Fig. 4 in the case of gamma-rays. Those results can be easily extended to the new models presented here, the main consequence being a smaller number of detectable sources.

V. CONTRIBUTION OF IMBHS TO THE EGB AND THEIR ANGULAR SPECTRUM

As we have seen in the previous sections, IMBHs are generically predicted in scenarios that seek to explain the existence of SMBHs at the centers of galaxies. It is therefore possible, in principle, that the gamma-ray flux from DM annihilations around IMBHs in all DM halos, and at all redshift, add together and contribute significantly to the diffuse Extra-galactic Gamma-ray Background (EGB) discovered by EGRET [62].

The origin of this gamma-ray emission is actually unknown, and although unresolved blazars are often considered as the most likely sources of the EGB, the most recent analysis suggest that they can not account for more than 25-50% of the measured EGB [63]. Besides standard astrophysical sources, like galaxies or clusters of galaxies [64, 65, 66], DM annihilations have been extensively studied as possible candidates to explain the EGB emission [4, 67, 68, 69].

The contribution from cosmological DM halos to the EGB is constrained to be rather low, in order to satisfy the observational bounds at the center of our Galaxy [70], even when the effect of spikes around SMBHs is taken into account. The presence of cosmological DM clumps could enhance the signal but according to the most recent results from DM simulations the expected boost factors

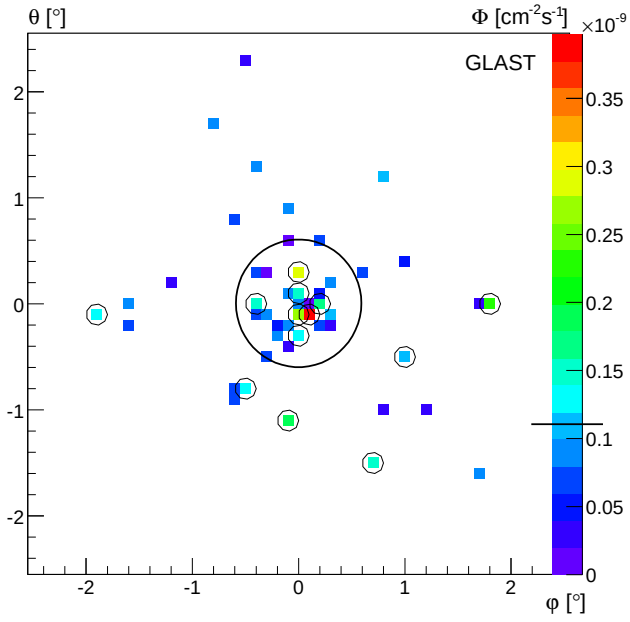

FIG. 5: Map of the gamma-ray flux in units of photons $\mathrm{cm}^{-2}\mathrm{s}^{-1}$, from DM annihilations around IMBHs in the Andromeda galaxy M31, relative to one random realization of IMBHs in M31. The size of the bins is 0.1° and the threshold is 4 GeV as appropriate the best angular resolution of Fermi (still labeled as GLAST in the figure). The circles highlight IMBHs within the reach of Fermi for a 5σ detection in 2 months. The big circle shows for comparison the M31 scale radius r_s.

are small (see Refs. [71, 72] and also the results in Ref. [69]). A sizeable diffuse emission is instead produced by the population of unresolved DM clumps hosted in our Galaxy [69, 73].

As for IMBHs, they can account for a large fraction of the measured EGB [61]. The mean intensity as a function of the energy, $\langle I(E)_{DM} \rangle$ produced by DM annihilations in cosmological IMBHs is given by:

$$\langle I(E)_{DM} \rangle = \int \frac{cdz}{H(z)} W\left(E[1+z], z\right), \qquad (9)$$

where

$$W(E,z) = \frac{(\sigma v)}{8\pi m_\chi^2} \frac{dN_\gamma}{dE}\left(E[1+z]\right) e^{-\tau(E[1+z],z)} \Delta^2(z). \qquad (10)$$

and the optical depth τ parametrizes the gamma-ray attenuation due to interactions with the extra-galactic background light (see e.g. Ref. [74]).

The factor $\Delta^2(z)$ in Eq. 10 contains the information on the DM spike profile ρ_{sp} around each IMBH and the comoving number density $n(z)$:

$$\Delta^2(z) = n(z) \int_{r_{cut}}^{r_{sp}} \rho_{sp}^2(r) d^3 r. \qquad (11)$$

The latter input cannot be computed in a straightforward manner using our current simulation techniques, but it can be modeled in an approximate manner based upon their results. For example, the BH formation models assume that initial BH formation is peaked at a certain redshift, z_f, to a good approximation, and is effective only in DM halos with masses above a certain threshold M_{thr}. These two parameters depend upon the specific formation scenario. Following this prescription and employing the halo mass function $dn/dM(M,z)$ predicted from extended Press-Schechter theory [75], the comoving number density at the formation redshift is:

$$n(z_f) = \int_{M_{thr}}^{\infty} dM \frac{dn}{dM}(M, z = z_f), \qquad (12)$$

where it is conservatively assumed that only one IMBH is formed per halo.

The number of IMBHs in present halos depend on the formation history of the host halo and is affected by the occurrence of BHs mergers. In good approximation it follows a linear dependence on the mass of the host halo, with a normalization N_{bh} for the Milky Way that is obtained from simulations. The present IMBHs comoving number density is thus:

$$n(0) = \int_{M_{min}}^{\infty} dM \frac{dn}{dM}(M, z = 0) N_{bh} \frac{M}{M_{MW}}. \qquad (13)$$

For a generic redshift z the IMBHs comoving number density can be parameterized assuming a power-law behavior which interpolates the BH number density at the formation redshift and at $z = 0$: $n(z) = n(z_f)\left[(1+z)/(1+z_f)\right]^\beta$.

With this recipe and based on the results of the simulation of Ref. [9] the authors in Ref. [61] computed the contribution of IMBHs to the EGB for the two IMBHs formation scenarios presented in Sec. II and for different choices of DM particle physics properties. In Fig. 6, we show that in the conservative case of scenario A the expected signal is largely below the EGB measurements. However, for scenario B the predicted diffuse emission is at the level of EGRET observations already for a standard particle physics setup, e.g. assuming a "thermal" annihilations cross section $\langle \sigma v \rangle = 3 \times 10^{-26} \mathrm{cm}^3\mathrm{s}^{-1}$ and $m_\chi = 100$ GeV.

As with the number of Galactic IMBHs, these predictions are subject to relatively large astrophysical uncertainties. Nonetheless, it is remarkable that models with astrophysical and particle physics parameters that have been fixed for independent reasons, the DM signal from cosmological IMBHs is comparable with the EGB flux extracted from EGRET observations. Of course, in order to detect effectively DM annihilations in the EGB it is necessary to distinguish the DM signal from other astrophysical emissions, such as that originated by blazars. Unfortunately, this is a difficult program to pursue using only spectral information, unless the DM signal is accompanied by striking spectral features, like those induced by

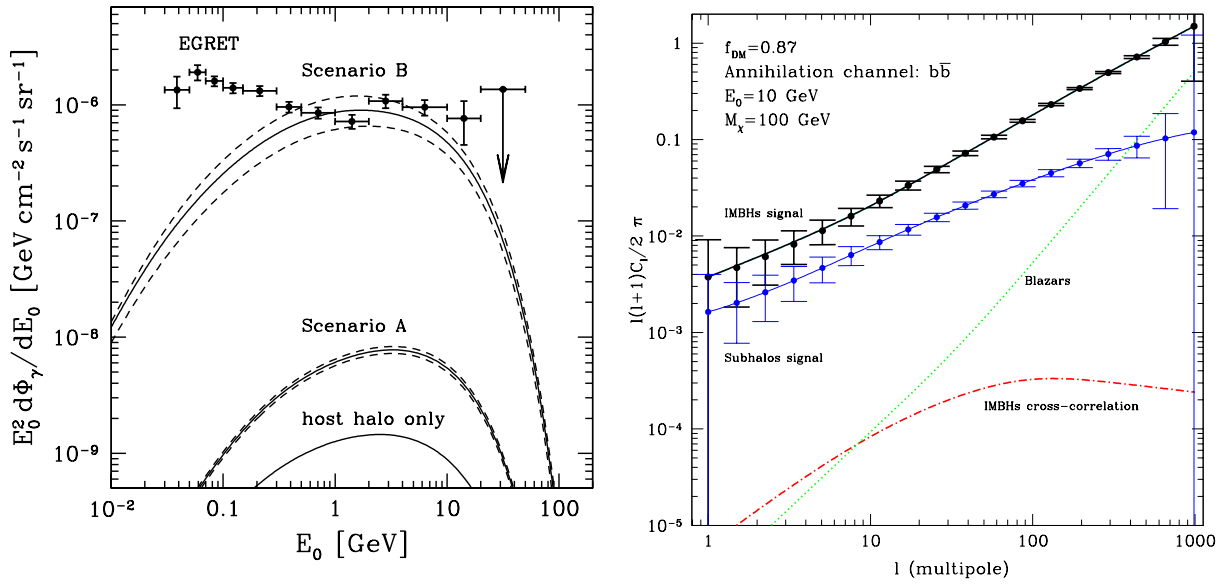

FIG. 6: *Left:* Contribution to the EGB from DM annihilations around IMBHs for scenario A and B. $m_\chi = 100$ GeV, $\langle\sigma v\rangle = 3\times10^{-26}\mathrm{cm}^3\mathrm{s}^{-1}$ and DM annihilations into $b\bar{b}$ have been considered. Taken from [61]. *Right:* Angular power spectrum of the EGB from DM annihilations around IMBHs at an energy $E_0 = 10$ GeV. The dashed line shows the DM contribution, the dotted one is for unresolved blazars and the dot-dashed is the cross-correlation term. The black solid line is the total signal and the error bars are for 2-years of Fermi data. The solid blue is the signal for DM annihilations in subhalos. Taken from [10].

gamma-ray line emission (see Ref. [61] for computations in IMBHs scenarios).

This problem can however be overcome by studying the angular correlations of the diffuse extra-galactic emission, as in Ref. [76]. In fact, the angular power spectrum of anisotropies from DM annihilations and from blazars are different, due to their different spatial distribution, energy spectra and radial emissivity profiles. Later on, other papers computed the angular spectrum of the EGB in the case that a substantial amount of the average EGB flux is accounted by DM annihilations in extra-galactic halos and subhalos [77] or in Galactic DM clumps [73], or considering both the contributions [69]. In all cases, if DM plays a role in the EGB, the analysis of the angular power spectrum of gamma-ray anisotropies can nicely detect its contribution and with the soon-available full-sky data by Fermi this approach will be testable.

In the case of IMBHs, the authors of Ref. [10] focused on scenario B and computed the angular power spectrum induced by DM annihilations around IMBHs. We refer to the original reference for details on the computations. As shown in Fig. 6 the shape of the angular power spectrum should help in distinguishing the DM signal from the blazar contribution to the EGB. These results refer to an energy of observations of $E_0 = 10$ GeV, which is a good compromise between maximization of the photon count and minimization of the Galactic foreground, which tends to masquerade the extra-galactic emission. In addition, natural DM candidates of around 100 GeV produce the largest gamma-ray yield at these energies. In order to assess more precisely the prospects for DM detection in the EGB they considered the unresolved blazar contribution as a known background, motivated by the fact that it should be modeled quite accurately from the future Fermi catalog of detected blazars. In addition, the power spectrum from unresolved blazars should be energy independent, due to the power-law energy dependence of their energy spectra and therefore it could be calibrated at low energies, where the contribution of DM annihilations is negligible and then subtracted from the total anisotropy data. After modeling the blazars contribution to the EGB, if it is assumed that the remaining fraction f_{DM} of the EGB flux at the energy of observation E_0 is due to DM annihilations, the signal C_l^s depends on the DM power spectrum C_l^{DM} and on the cross correlation between the DM and blazars signals C_l^{Cr}:

$$C_l^s = f_{DM}^2 C_l^{DM} + 2 f_{DM}(1-f_{DM}) C_l^{Cr}. \qquad (14)$$

Fig. 6 shows the signal as well as the projected 1σ error bars after two years of Fermi observations. The prospects for distinguishing the signal of DM annihilation around IMBHs in the angular EGB power spectrum are encouraging. This conclusion holds for different choices of DM mass and annihilation channel and energy of detection, provided that DM annihilations substantially contribute to the EGB at E_0, i.e. for $f_{DM} \gtrsim 0.3$. Moreover, if the DM signal is dominated by DM emission in cosmological subhalos instead that around IMBHs, the predicted angular power spectrum is different and for sizeable values

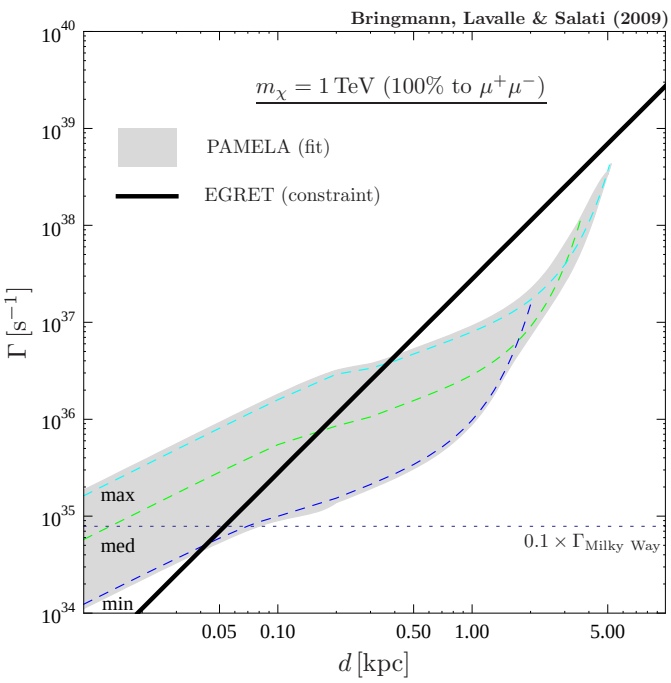

FIG. 7: The solid line show the constraint in the DM annihilation rate $\Gamma = 1/2\langle\sigma v\rangle/m_\chi^2 \int d\mathbf{x}\rho_{sp}(\mathbf{x})$ of a nearby DM overdensity at a distance d from the Earth. The shaded area shows the combinations of $\Gamma - d$ needed to explain the PAMELA positron excess. The dashed lines refers to a set of propagation parameters defined in Ref. [79]. For comparison the dotted line indicates the 10% of Γ for the whole MW assuming $\langle\sigma v\rangle = 3 \times 10^{-26}\mathrm{cm}^{-3}\mathrm{s}^{-1}$. Taken from [80].

of f_{DM} the two scenarios should be distinguishable by Fermi observations.

VI. DISCUSSION AND CONCLUSIONS

Indirect DM searches have received a lot of attention recently, in large part due to the recent results of experimental collaborations such as Fermi, PAMELA, HESS and others. However, unless unambiguous spectral features are detected [78], it will be difficult to discriminate any incident flux of high-energy particles from astrophysical sources (either known or unknown) and identify a signal due to DM annihilation. The mini-spikes scenario discussed here may provide an interesting solution to this problem.

In fact, in the previous sections we have shown that IMBHs are promising targets for DM indirect detection, as a consequence of the large DM overdensities produced around them by gravitational processes during the formation of the BH. The properties of these objects and the distribution of DM about these objects both depend on the unknown BH formation mechanism. In Ref. [9] the authors investigated in detail two astrophysical models proposed in the contemporary literature. This study utilized numerical simulations to make predictions for the population of IMBHs that should be present in our Galaxy today. These objects could appear as bright gamma-ray emitters as a consequence of the DM annihilations occurring in the dense DM spikes. Indeed the prospects for detecting such objects with Fermi and Air Cherenkov Telescopes are encouraging. A spectacular signature for a DM signal may come from the detection of a class of gamma-ray point sources that are not associated with astrophysical sources and that share the same energy spectrum. IMBHs may also be detected through neutrinos or they can produce a sizable excess in antimatter cosmic-ray fluxes, as studied in Ref. [81]. Moreover, analogous populations of IMBHs should be present in other galaxies, such as the nearby Andromeda galaxy and several gamma-ray sources could be detectable.

In general, the gamma-ray fluxes from IMBHs in all DM halos at all redshifts produce a diffuse gamma-ray background that for the most optimistic scenario B can explain a large fraction of the observed EGB. This opens the interesting possibility to detect DM annihilations in the extra-galactic background. The best strategy would be to analyze not only the EGB energy spectrum but also the angular correlations of the emission. In fact, the EGB angular power spectrum could provide a robust method to distinguish the DM signal from conventional astrophysical emission.

In Ref. [80], the authors derived constraints on the mini-spike scenario from a comparison of predictions based on BZS models with EGRET data. These authors claim that they rule out the possibility to detect the products of DM annihilation in mini-spikes. Despite the bold claim, their analysis only rules out a specific combination of cosmological and astrophysical parameters, for only one (out of many) possible formation scenarios. Actually, we showed above that by simply adopting the WMAP 5-year cosmological parameters, the expected number of objects went down by a factor of 2, and that changing the redshift of formation in scenario A, and of ionization in scenario B, substantially modifies the predicted number of sources. Moreover, Figs. 3 and 4 show that one can obtain quite optimistic prospects for Fermi (with up to ~ 200 sources in reach of detection) even assuming no detection by EGRET.

Still, the constraints of Ref. [80] are extremely useful. In particular, these results bear on the possible implications of the mini-spikes scenario for the recent measurements of the positron and electron flux at high energy [82, 83]. The possibility that mini-spikes boost the annihilation signal thus providing the appropriate normalization of the positron flux is found to be viable, as shown in Fig. 7, and it would be interesting to see whether such a result holds for updated mini-spikes models. This would allow to circumvent the multi-messenger constraints (see, e.g., Refs. [84, 85]).

In conclusion, the mini-spike scenario provides the opportunity to discover a new population of sources (IMBHs) and DM annihilations at the same time. The

most prominent predicted signature of this scenario is unmistakable: the observation of many point-like sources, not correlated with the Galactic disk, with an identical spectrum. It is therefore important, despite the various constraints and the many astrophysical uncertainties, to search for this population of objects in present and upcoming data, especially those of the gamma-ray satellite Fermi.

[1] P. J. E. Peebles, Astrophys. J. **178** (1972) 371
[2] P. Young Astrophys. J. **242** (1980) 1232
[3] P. Gondolo and J. Silk, Phys. Rev. Lett. **83** (1999) 1719 [arXiv:astro-ph/9906391].
[4] P. Ullio, H. Zhao and M. Kamionkowski, Phys. Rev. D **64** (2001) 043504 [arXiv:astro-ph/0101481].
[5] D. Merritt, M. Milosavljevic, L. Verde and R. Jimenez, Phys. Rev. Lett. **88** (2002) 191301 [arXiv:astro-ph/0201376].
[6] G. Bertone and D. Merritt, Phys. Rev. D **72** (2005) 103502 [arXiv:astro-ph/0501555].
[7] G. Bertone and D. Merritt, Mod. Phys. Lett. A **20** (2005) 1021 [arXiv:astro-ph/0504422].
[8] H. S. Zhao and J. Silk, Phys. Rev. Lett. **95** (2005) 011301 [arXiv:astro-ph/0501625].
[9] G. Bertone, A. R. Zentner and J. Silk, Phys. Rev. D **72** (2005) 103517 [arXiv:astro-ph/0509565].
[10] M. Taoso, S. Ando, G. Bertone and S. Profumo, arXiv:0811.4493 [astro-ph].
[11] C. L. Fryer and V. Kalogera, Astrophys. J. **554** (2001) 548 [arXiv:astro-ph/9911312].
[12] D. A. Swartz, K. K. Ghosh, A. F. Tennant and K. W. Wu, arXiv:astro-ph/0405498.
[13] M. C. Miller and E. J. M. Colbert, Int. J. Mod. Phys. D **13** (2004) 1 [arXiv:astro-ph/0308402].
[14] L. Ferrarese and H. Ford, arXiv:astro-ph/0411247.
[15] X. Fan *et al.* [SDSS Collaboration], Astron. J. **122** (2001) 2833 [arXiv:astro-ph/0108063].
[16] A. J. Bath, P. Martini, C. H. Nelson and L. C. Ho, Astrophys. J. **594** (2003) L95
[17] C. J. Willott, R. J. McLure and M. J. Jarvis, Astrophys. J. **587** (2003) L15 [arXiv:astro-ph/0303062].
[18] http://lisa.nasa.gov/
[19] S. M. Koushiappas and A. R. Zentner, Astrophys. J. **639** (2006) 7 [arXiv:astro-ph/0503511].
[20] E. E. Flanagan and S. A. Hughes, Phys. Rev. D **57** (1998) 4535 [arXiv:gr-qc/9701039].
[21] E. E. Flanagan and S. A. Hughes, Phys. Rev. D **57** (1998) 4566 [arXiv:gr-qc/9710129].
[22] P. Madau and M. J. Rees, Astrophys. J. **551** (2001) L27 [arXiv:astro-ph/0101223].
[23] T. Abel, G. L. Bryan and M. L. Norman, Astron. Astrophys. **540** (2000) 39 [arXiv:astro-ph/0002135].
[24] V. Bromm, P. S. Coppi and R. B. Larson, Astrophys. J. **564** (2002) 23 [arXiv:astro-ph/0102503].
[25] A. Heger, C. L. Fryer, S. E. Woosley, N. Langer and D. H. Hartmann, Astrophys. J. **591** (2003) 288 [arXiv:astro-ph/0212469].
[26] Bond, J. R., Arnett, W. D., & Carr, B. J. Astrophys. J. **280** (1984) 825
[27] C. L. Fryer, S. E. Woosley and A. Heger, Astrophys. J. **550** (2001) 372 [arXiv:astro-ph/0007176].
[28] R. B. Larson, arXiv:astro-ph/9912539.
[29] R. Schneider, A. Ferrara, B. Ciardi, V. Ferrari and S. Matarrese, Mon. Not. Roy. Astron. Soc. **317** (2000) 385 [arXiv:astro-ph/9909419].
[30] S. M. Koushiappas, J. S. Bullock and A. Dekel, Mon. Not. Roy. Astron. Soc. **354** (2004) 292 [arXiv:astro-ph/0311487].
[31] M. G. Haehnelt & M. J. Rees, Mon. Not. Roy. Astron. Soc. **263** (1993) 168.
[32] A. Loeb & F. A. Rasio, Astrophys. J. **432** (1994) 52.
[33] D. J. Eisenstein & A. Loeb, Astrophys. J. **443** (1995) 11
[34] M. G. Haehnelt, P. Natarajan & M. J. Rees, Mon. Not. Roy. Astron. Soc. **300** (1998) 817
[35] O. Y. Gnedin, arXiv:astro-ph/0108070.
[36] V. Bromm and A. Loeb, Astrophys. J. **596** (2003), 34 [arXiv:astro-ph/0212400].
[37] A. R. Zentner and J. S. Bullock, Astrophys. J. **598** (2003) 49 [arXiv:astro-ph/0304292].
[38] A. R. Zentner, A. A. Berlind, J. S. Bullock, A. V. Kravtsov and R. H. Wechsler, Astrophys. J. **624** (2005) 505 [arXiv:astro-ph/0411586].
[39] S. M. Koushiappas, A. R. Zentner and T. P. Walker, Phys. Rev. D **69** (2004) 043501 [arXiv:astro-ph/0309464].
[40] J. F. Navarro, C. S. Frenk and S. D. M. White, Astrophys. J. **490** (1997) 493 [arXiv:astro-ph/9611107].
[41] M. Fornasa and G. Bertone, Int. J. Mod. Phys. D **17** (2008) 1125 [arXiv:0711.3148 [astro-ph]].
[42] G. D. Quinlan, L. Hernquist and S. Sigurdsson, arXiv:astro-ph/9407005.
[43] S. Sigurdsson, arXiv:astro-ph/0303311.
[44] J. D. MacMillan and R. N. Henriksen, Astrophys. J. **569** (2002) 83 [arXiv:astro-ph/0201153].
[45] D. Merritt, S. Harfst and G. Bertone, Phys. Rev. D **75** (2007) 043517 [arXiv:astro-ph/0610425].
[46] E. Komatsu *et al.* [WMAP Collaboration], Astrophys. J. Suppl. **180** (2009) 330 [arXiv:0803.0547 [astro-ph]].
[47] K. Griest and D. Seckel, Phys. Rev. D **43** (1991) 3191.
[48] A. Sommerfeld, Annalen der Physik **403** (1931) 257
[49] J. Hisano, S. Matsumoto and M. M. Nojiri, Phys. Rev. Lett. **92** (2004) 031303 [arXiv:hep-ph/0307216].
[50] M. Cirelli, A. Strumia and M. Tamburini, Nucl. Phys. B **787** (2007) 152 [arXiv:0706.4071 [hep-ph]].
[51] M. Lattanzi and J. I. Silk, arXiv:0812.0360 [astro-ph].
[52] M. Kamionkowski and M. S. Turner, Phys. Rev. D **42** (1990) 3310.
[53] R. Catena, N. Fornengo, A. Masiero, M. Pietroni and F. Rosati, Phys. Rev. D **70** (2004) 063519 [arXiv:astro-ph/0403614].
[54] G. Gelmini, P. Gondolo, A. Soldatenko and C. E. Yaguna, Phys. Rev. D **74** (2006) 083514 [arXiv:hep-ph/0605016].
[55] F. Aharonian *et al.* [HESS Collaboration], Phys. Rev. D **78** (2008) 072008 [arXiv:0806.2981 [astro-ph]].
[56] G. Bertone, T. Bringmann, R. Rando, G. Busetto and A. Morselli, arXiv:astro-ph/0612387.
[57] E. A. Baltz *et al.* [FERMI-LAT Collaboration], JCAP **0807** (2008) 013 [arXiv:0806.2911 [astro-ph]].
[58] M. Fornasa, M. Taoso and G. Bertone, Phys. Rev. D **76** (2007) 043517 [arXiv:astro-ph/0703757].

[59] G. Bertone, Phys. Rev. D **73** (2006) 103519 [arXiv:astro-ph/0603148].
[60] G. Bertone, New Astron. Rev. **51** (2007) 321.
[61] S. Horiuchi and S. Ando, Phys. Rev. D **74** (2006) 103504 [arXiv:astro-ph/0607042].
[62] P. Sreekumar *et al.* [EGRET Collaboration], Astrophys. J. **494** (1998) 523 [arXiv:astro-ph/9709257].
[63] T. Narumoto and T. Totani, Astrophys. J. **643** (2006) 81 [arXiv:astro-ph/0602178].
[64] H. Liang, V. Dogiel and M. Birkinshaw, Mon. Not. Roy. Astron. Soc. **337** (2002) 567 [arXiv:astro-ph/0208509].
[65] Y. Rephaeli, J. Nevalainen, T. Ohashi and A. M. Bykov, arXiv:0801.0982 [astro-ph].
[66] V. Pavlidou and B. D. Fields, Astrophys. J. **575** (2002) L5 [arXiv:astro-ph/0207253].
[67] L. Bergstrom, J. Edsjo and P. Ullio, Phys. Rev. Lett. **87** (2001) 251301 [arXiv:astro-ph/0105048].
[68] J. E. Taylor and J. Silk, Mon. Not. Roy. Astron. Soc. **339** (2003) 505 [arXiv:astro-ph/0207299].
[69] M. Fornasa, L. Pieri, G. Bertone and E. Branchini, arXiv:0901.2921 [astro-ph].
[70] S. Ando, Phys. Rev. Lett. **94** (2005) 171303 [arXiv:astro-ph/0503006].
[71] J. Diemand, M. Kuhlen, P. Madau, M. Zemp, B. Moore, D. Potter and J. Stadel, Nature 454 (2008) 735 arXiv:0805.1244 [astro-ph].
[72] V. Springel *et al.*, arXiv:0809.0894 [astro-ph].
[73] J. M. Siegal-Gaskins, JCAP **0810** (2008) 040 [arXiv:0807.1328 [astro-ph]].
[74] M. H. Salamon and F. W. Stecker, Astrophys. J. **493** (1998) 547 [arXiv:astro-ph/9704166].
[75] R. K. Sheth and G. Tormen, Mon. Not. Roy. Astron. Soc. **308** (1999) 119 [arXiv:astro-ph/9901122].
[76] S. Ando and E. Komatsu, Phys. Rev. D **73** (2006) 023521 [arXiv:astro-ph/0512217].
[77] S. Ando, E. Komatsu, T. Narumoto and T. Totani, Phys. Rev. D **75** (2007) 063519 [arXiv:astro-ph/0612467].
[78] L. Bergstrom and P. Ullio, Nucl. Phys. B **504**, 27 (1997) [arXiv:hep-ph/9706232]; Z. Bern, P. Gondolo and M. Perelstein, Phys. Lett. B **411**, 86 (1997) [arXiv:hep-ph/9706538]; P. Ullio and L. Bergstrom, Phys. Rev. D **57**, 1962 (1998) [arXiv:hep-ph/9707333]; L. Bergstrom, P. Ullio and J. H. Buckley, Astropart. Phys. **9**, 137 (1998) [arXiv:astro-ph/9712318]. G. Bertone, C. B. Jackson, G. Shaughnessy, T. M. P. Tait and A. Vallinotto, arXiv:0904.1442 [astro-ph.HE]. L. Bergstrom, T. Bringmann, M. Eriksson and M. Gustafsson, Phys. Rev. Lett. **94**, 131301 (2005) [arXiv:astro-ph/0410359]; A. Birkedal, K. T. Matchev, M. Perelstein and A. Spray, arXiv:hep-ph/0507194, J. F. Beacom, N. F. Bell and G. Bertone, Phys. Rev. Lett. **94** (2005) 171301 [arXiv:astro-ph/0409403].
[79] T. Delahaye, F. Donato, N. Fornengo, J. Lavalle, R. Lineros, P. Salati and R. Taillet, arXiv:0809.5268 [astro-ph].
[80] T. Bringmann, J. Lavalle and P. Salati, arXiv:0902.3665 [astro-ph.CO].
[81] T. Bringmann and P. Salati, Phys. Rev. D **75** (2007) 083006 [arXiv:astro-ph/0612514].
[82] O. Adriani *et al.* [PAMELA Collaboration], arXiv:0810.4995 [astro-ph].
[83] J. Chang *et al.*, Nature **456**, 362 (2008).
[84] G. Bertone, M. Cirelli, A. Strumia and M. Taoso, arXiv:0811.3744 [astro-ph].
[85] L. Bergstrom, G. Bertone, T. Bringmann, J. Edsjo and M. Taoso, arXiv:0812.3895 [astro-ph].